Measurements of radiation near an atomic spectral line from the interaction of a 30 GeV electron beam and a long plasma

P. Catravas, S. Chattopadhyay, E. Esarey, and W. P. Leemans
Lawrence Berkeley National Laboratory, University of California, Berkeley, California 94720

R. Assmann,* F.-J. Decker, M. J. Hogan, R. Iverson, R. H. Siemann, D. Walz, and D. Whittum
Stanford Linear Accelerator Center, Stanford University, Stanford, California 94309

B. Blue, C. Clayton, C. Joshi, K. A. Marsh, W. B. Mori, and S. Wang
University of California Los Angeles, Los Angeles, California 90095

T. Katsouleas, S. Lee, and P. Muggli
University of Southern California, Los Angeles, California 90089
(Received 31 October 2000; published 20 September 2001)

Emissions produced or initiated by a 30-GeV electron beam propagating through a ~1-m long heat pipe oven containing neutral and partially ionized vapor have been measured near atomic spectral lines in a beam-plasma wakefield experiment. The Cerenkov spatial profile has been studied as a function of oven temperature and pressure, observation wavelength, and ionizing laser intensity and delay. The Cerenkov peak angle is affected by the creation of plasma, and estimates of neutral and plasma density have been extracted. Increases in visible background radiation, consistent with increased plasma recombination emissions due to dissipation of wakefields, were simultaneously measured.

DOI: 10.1103/PhysRevE.64.046502 PACS number(s): 41.75.Ht, 52.40.Mj

I. INTRODUCTION

Intense electron beam-plasma interactions have applications to advanced accelerators [1–3], plasma lenses [4], and radiation sources such as ion channel lasers [5] and wake radiation from magnetized plasmas [6]. Plasma accelerators are studied as alternatives to conventional RF accelerators as they can provide accelerating gradients that are several orders of magnitude larger. The wakefield amplitude is maximized when the length of the driving (electron or laser) pulse, L, is on the order of the plasma wavelength, λ_p, where $\lambda_p = 2\pi c/\omega_p$, $\omega_p = \sqrt{N_e e^2/m_e \epsilon_0}$, and N_e is the electron plasma density [1]. For drive beams with a duration of 0.1–1 ps, the corresponding plasma densities are 10^{17}–10^{15} cm^{-3}. As the coupling between the drive beam and plasma is largely determined by N_e, its measurement is an essential aspect of plasma accelerators.

Radiation, such as Cerenkov radiation (CR), optical transition radiation (OTR), and recombination radiation (RR), produced or initiated by the electron beam (e beam) can provide an opportunity to measure the plasma and wake properties. CR has been widely applied in high energy physics for particle identification, through use of the Cerenkov cutoff condition, $\gamma^{-2} + \theta_c^2 \sim 2(n-1)$ (small angles), which depends on the electron velocity, v, where $\gamma = (1 - v^2/c^2)^{-1/2}$, n is the index of refraction of the medium, and θ_c is the CR cone angle. In contrast to the usual implementations, we operate in the limit $\gamma^{-2} \ll n-1$, which allows measurement of the properties of the medium, rather than the e beam. CR [7] is produced when the speed of light in the medium, c/n, is less than that of the electrons. The index of refraction of the medium, neglecting absorption, can be modeled by

$$n - 1 \sim \sum_{species,s} \frac{N_s e^2 f_{ik}}{2 m_e \epsilon_0 (\omega_{res}^2 - \omega^2)} - \frac{N_e}{2 N_{cr}}, \qquad (1)$$

where N_s is the species density (neutrals and/or ions), f_{ik} is the oscillator strength, ω_{res} is the frequency of the atomic resonance, and $N_{cr} = \omega^2 m_e \epsilon_0 / e^2$ is the critical density at the observation frequency ω. Expressions for the spectral flux density and photon levels of CR can be found in standard texts [7].

In this paper, we present experimental results on a diagnostic method involving the interaction of relativistic beams with media (neutral and partially ionized gas, plasmas, and thin foils). Experiments on neutral and plasma density measurements in a Li oven are described, with operation on the long wavelength side of an atomic spectral resonance so as to allow CR emission. CR is then produced with an intensity distribution that is peaked at the phase matched cone angle, $\theta_c^2 \sim 2(n-1)$ (small angles), and can provide a measure of changes in N_s (i.e., due to ionization), N_e, and ω_{res} on the timescale of the e beam bunchlength.

These results are of interest to the research area of advanced accelerators and radiation sources, as well as other fields. The generation of Cerenkov radiation near x-ray resonances has been proposed as a short pulse x-ray source [8,9]. The high electric and magnetic fields, such as present in the

*Present address: CERN, European Organization for Nuclear Research, Geneva, Switzerland.

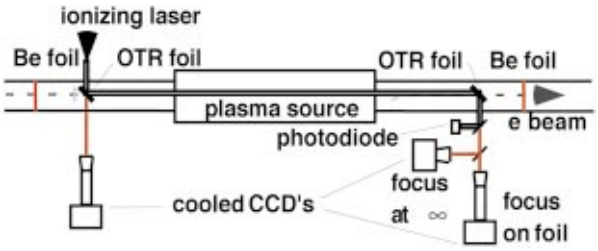

FIG. 1. (Color) Experimental setup.

reported experiment (or in other plasma wakefield accelerator experiments at lower energy), along with the near resonance radiation generated in the experiments, could be used by atomic physicists studying the physics of atoms in ultrahigh intensity fields. Finally, the Cerenkov radiation near atomic spectral lines has been studied in high energy astrophysics [10].

II. EXPERIMENTAL SETUP

In the *E*157 plasma wakefield acceleration experiment [3] at the Stanford Linear Accelerator Final Focus Test Beam, a 2 ps (rms) long, 30-GeV *e*-beam bunch with 2×10^{10} particles in a 30–100 μm spot traverses a Li heat pipe [11] oven (Fig. 1). In this scheme, the electron bunch blows out plasma electrons, producing transverse focusing forces along the bunch (that lead to betatron oscillations in the *e*-beam envelope) and longitudinal accelerating forces as the plasma electrons return at the electron bunch tail. The design value of plasma density, 2×10^{14} cm^{-3}, was chosen to optimize both the longitudinal field and the fraction of the tail electrons that can experience acceleration.

Measurements described below were taken with two ovens, one of Li column length 1.35 m [12], plugged by He at a partial pressure of 450 mTorr, the other of length 1 m with 200 mTorr He [13]. The Li neutral density was typically $\sim10^{15}$ cm^{-3}. An ArF excimer laser operating at 193 nm (UV) partially ionized the Li [12,13]. The UV was incoupled and outcoupled by dielectric coated fused Silica foils, 150 μm thick, separated by 2.5 m. The opposite side of the foil was coated with Al for *e*-beam spot size monitoring using OTR [14]. Images of the downstream foil and far field (focus at infinity) radiation intensity profiles upstream and downstream were measured with 14 and 16 bit cooled CCD's. The plasma density seen by the *e* beam was changed by varying the time between laser and *e*-beam injection.

III. EXPERIMENTAL RESULTS AND ANALYSIS

A. Neutral density diagnosis

To benchmark the CR component against theory, initial measurements were done on propagating the *e* beam through He and neutral Li. The observed radiation on the downstream foil (see Fig. 1) consisted of OTR and CR. OTR from the 30 GeV beam had been previously studied for spot size and divergence measurements [14] and is well understood. First, the *e* beam was propagated in a He-filled oven at room temperature. Analysis of the observed ringlike radiation pattern (at 676.4 nm, far separated from the He ground state atomic resonance of 58.4 nm) resulted in a density that agreed to within 10% with the density given by the ideal gas law at 100 Torr and 400 Torr.

In the Li-filled heat pipe oven, in which the Li column is confined by two short He plugs, concentric cones corresponding to the Li and He regions were observed [Fig. 2(a)]. Far field images recorded from 676.4 nm (1.5 nm BW) to <670.8 nm (the Li ground state resonance wavelength) are shown in Fig. 2(b). We observed: (i) disappearance of CR from Li on the short wavelength side of the resonance, where the index of refraction drops below v/c, (ii) increase in cone radius, and (iii) increase in the cone width as the observation wavelength approaches the spectral line. CR cones from Li were compared at 800 nm, 700 nm, and 676.4 nm and, despite the increasing proximity to the spectral resonance, yielded estimates of neutral density that agreed within 7%.

CR was also recorded during oven cool down to study the dependence of the CR cone angle θ_c on oven temperature, T, and pressure. The measured He plug pressure was 270 mTorr for the scan in Fig. 3, giving N_n of 2.6×10^{15} cm^{-3} from pressure balance in ''oven mode.'' At the operating temperature, the neutral density estimated from the CR cone was 2.1×10^{15} cm^{-3}, in reasonable agreement with pressure balance. The neutral density scaling with T as the Li vapor changes state is $N_n=N_o(T_o/T)\exp(-r_o/RT)$, where r_o is the heat of vaporization, R is the universal gas constant, and N_o is the density at the temperature T_o. N_n estimated from θ_c vs T is plotted in Fig. 3 along with known values [15]. Cone peak angles were calibrated using far field measurements. The heat of vaporization, r_o, determined from the slope of Fig. 3(b) came within 5–10% of the known value for Li, 148.13 kJ/mol [15] both at 676 and 700 nm [16].

B. Observation of radiation in the presence of plasma

The dependence of the CR spatial profile on plasma production was studied at 676 nm by scanning the relative delay

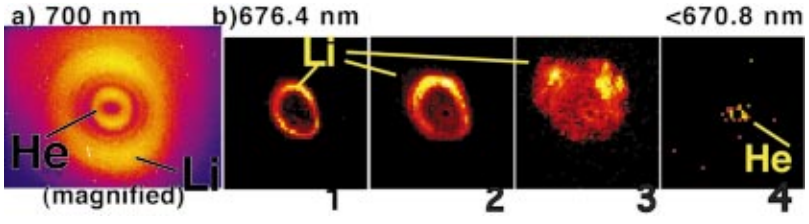

FIG. 2. (Color) (a) Far field image (537 °C) shows separate cones for the Li and He regions. (b) Far field wavelength scan from 676 nm through and below the resonance shows disappearance of Li CR cone, and trends in cone radius and width. Wavelength decreases from left to right. Dispersive effects have broadened the cone radius and width in frame 3. The asymmetry in (b) is due to the surface irregularity of a splitting pellicle added to the system.

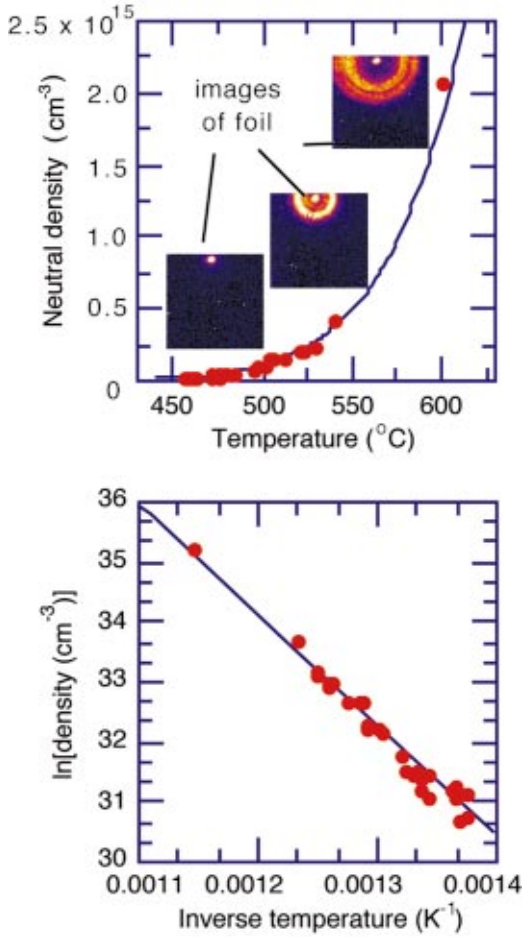

FIG. 3. (Color) (a) Neutral density estimated from CR and (b) its functional dependence are plotted for an oven cool down. The solid lines are known vaporization curves [15].

Δt between the e beam and the ionizing laser by up to 50 μs, (i.e., a few plasma decay times). Two strong effects were observed. First, θ_c shifted inward in the presence of plasma. Second, the CR cone was riding on a substantial background signal, which appeared in the presence of plasma, with an intensity dependent on wavelength, time delay Δt, and coalignment.

Figure 4(a) shows the images of a thin foil 1.33 m downstream from the oven center at 676 nm for delays Δt of 3.5 and 47.5 μs, after subtraction of the baseline radiation pattern from the red hot oven wick over a 0.5 s integration time. There are three constituents of these images: a CR cone, an OTR central spot, and background. Separation of the parts was done by incrementally subtracting images from consecutive timesteps, starting from laser off and working toward smaller delays, Δt. Once the slow varying component was quantified and removed, the spatially separate CR cone peak angle and OTR width were determined. The CR cone angle systematically decreased with decreasing delay (increasing plasma density). At the same time, the OTR images of the transverse profile of the e beam showed that the number of betatron oscillations executed by the e beam along the length of the oven decreased by about one oscillation as the plasma

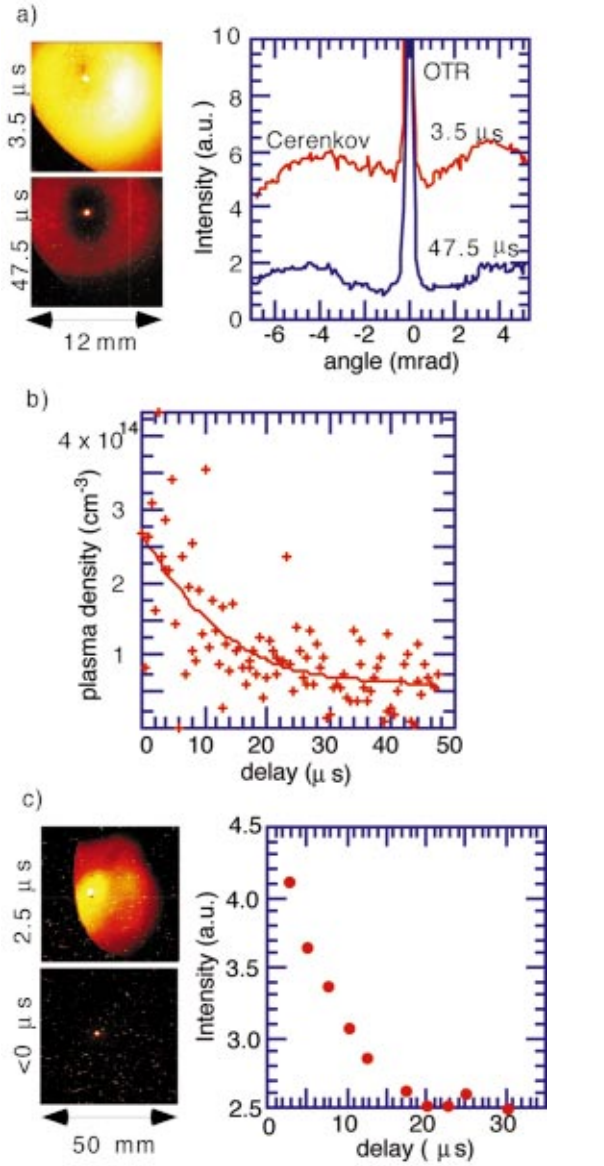

FIG. 4. (Color) Downstream foil data are shown for two wavelength ranges: (a),(b) 676.4 nm (1.35 m oven) and (c) 505 nm (1 m oven). (a) Images at high (3.5 μs delay) and low (47.5 μs delay) plasma density. Lineouts show inward shift of CR cone and increase in visible background level. (b) Plasma density estimated from inward shift of CR cone angle vs delay. (c) Images at $\Delta t<0$ and 2.5 μs delay show spatial extent of background and total intensity collected into 80 nm BW vs delay. The edge in the image taken at 2.5 μs delay is due to the 2 in. pellicle aperture.

density available immediately after laser fire decreased to that of 47 μs after laser fire. The e-beam spot size went through minima at delays of 6 and 37 μs. A maximum occurred at 14 μs; another maximum was being approached near zero delay. Substantial increases in the visible background appeared with decreasing delay with a time constant on the order of the plasma decay time. These observations are analyzed in more detail below.

Plasma density causes inward shifting of the CR cone. The fractional ionization, (N_i/N_n), where N_i is the ion den-

sity, can be quantified from θ_c when the observation wavelength is chosen sufficiently far from resonance so that shifts in ω_{res} can be neglected. A baseline measurement without plasma gives the initial neutral density. Depletion of the neutral population reduces the cone angle and the ratio to the baseline angle will be proportional to $\sqrt{1-N_i/N_n}$. The plasma density extracted from the CR cone radius is shown in Fig. 4(b). The estimated initial plasma density is 2.6×10^{14} cm^{-3}. The factor of 4 decrease in density of 35 μs is approximately the same as measured previously [12], but the two experiments have different detailed time dependencies.

The plasma density extracted from the CR cone can be compared with that required to produce the observed number of betatron oscillations in the OTR images of the *e*-beam spot size. The relation between plasma density and the betatron wavelength, λ_β, assuming that the plasma ions exert a linear restoring force on the *e* beam, is given by $\lambda_\beta = \sqrt{2\gamma}\lambda_p \propto N_e^{-1/2}$. Plasma density diagnosis based on measurement of betatron oscillations has been studied experimentally [17,18]. Including the transverse focusing over the plasma column length and adding the short drift space to the OTR foil, the spot size at the foil was calculated as a function of plasma density. Notice that for this analysis, given the plasma density that remained at 47 μs according to Fig. 4(b), a spot size minimum at delay greater than 50 μs is expected, implying that the two pinches recorded during the scan were the second and third pinch. The observed betatron oscillations can be modeled using initial plasma densities $1-2\times10^{14}$ cm^{-3} and assuming a flat top Li profile with lengths of 1.4–1.0 m. The nominal oven length was 1.35 m, so the latter result would imply either that the effective length of the plasma column was shorter (which could result if the ionizing laser was not perfectly collimated or if the oven was not in oven mode when these measurements were made) or that there is roughly 50% disagreement between these two measurements of plasma density.

The CR cone radius was also studied as a function of the ionizing laser energy near zero delay. The extracted plasma density was linear with UV fluence. The plasma density extracted from CR [Fig. 4(b)] is consistent with plasma density estimated from UV absorption assuming a 1×3-mm spot size, 0.72-mJ incident energy at the plasma, and 14% fractional ionization.

The dependence of the background intensity on incident UV fluence and delay at 676 nm was studied. In both cases, the background increased linearly with the plasma density extracted from the CR cone shift. The timing dependence of the total number of intercepted photons was compared at different wavelengths, 700 nm (40 nm BW, 1% transmission at 670.8 nm), 676.4 nm (1.5 nm BW, 1.7% transmission at 670.8 nm), 632 nm (1 nm BW), and 505 nm (80 nm BW). The background intensity was strong for the 676.4 nm and 505 nm filters, intermittent for the 700 nm filter, but dropped by three orders of magnitude at 632 nm.

The use of a 505 nm filter provided measurement of background radiation without additional contributions either from Li CR or from RR near 670.8 nm. The measurements with the 505 nm filter were taken with the 1 m oven [13]. In Fig. 4(c), the spatial profiles are compared for negative delay (*e* beam arrives before laser) and for 2.5 μs delay, along with the total intercepted intensity plotted against delay, Δt. (Note that this includes a constant contribution from OTR.) The background intensity was steering dependent; the intensity reduced and disappeared as the laser was pivoted upstream from the oven entrance to be out of alignment with the *e* beam.

We speculate that additional recombinations, due to wake energy dissipation through ionization and excitation of the medium, produced the increase in visible background radiation [19], which leaked through the tails in the filter spectral response. For design values of ~100 MeV lost per electron in the bulk of an *e* beam with $\sim10^{10}$ particles, the total stored energy in the wakefield is 3 orders of magnitude greater than that absorbed from the ionizing laser. Recombination light from the UV-ionized plasma only (*e* beam off) was recorded as the interference filter was tilted to pass through to the short wavelength side of the atomic spectral line. Because the integration time of the CCD camera is 0.5 s, much longer than the relative timing scan of 50–100 μs, recombination of plasma ionized by the UV laser alone cannot explain the delay-dependent effect.

The contribution of synchrotron radiation was considered because a systematic increase in *e*-beam steering with increasing plasma density was observed during the scan of Figs. 4(a) and 4(b), reaching a displacement of 300 μm at the OTR foil 1.33 m downstream from center of the plasma. This corresponds to a bending radius of curvature of $\sim4.4\times10^3$ m, or an angular deflection of 0.23 mrad of the *e*-beam trajectory by the plasma. However, the number of photons expected at 676 nm [20] is several orders of magnitude too low and the spatial characteristics are inconsistent with that observed. Similarly, the low flux and nearly uniform intensity distribution for visible wavelengths expected from betatron radiation was not a significant contribution.

In this paper, errors are typically a factor of two. Sources of error include background subtraction, filter tilts, nonuniform oven profiles, etc. Resonant wavelength shift due to the Stark or Zeeman effect were estimated to be less than 0.1 nm [21]. Comparison of the ratio of radii of CR cones at 676, 700, and 800 nm indicated that these shifts could indeed be neglected.

IV. CONCLUSIONS AND FUTURE WORK

In conclusion, measurements of radiation from a 30-GeV electron beam interacting with a meter long Li heat pipe oven near the 670.8 nm atomic spectral line of Li have been performed for a plasma wakefield experiment and provide opportunities for monitoring parameters important to the wakefield interaction. Cerenkov radiation was utilized in the limit where the beam energy contributes negligibly to the phase matched cone angle, which is consequently determined directly from the index of refraction of the medium. Neutral density was extracted from the Cerenkov radiation spatial profile in agreement with the Li vapor pressure curve. The Cerenkov phase matched cone angle responded to the presence of plasma. Plasma density estimated from the Cer-

enkov cone angle is in rough agreement with an independent calibration of the plasma density obtained from simultaneous measurements of betatron oscillations downstream from the plasma. Strong increases in the visible background levels were observed near atomic spectral lines, consistent with wakefield energy dissipation through excitation and recombination in the medium.

In a future experiment, the error bars on the measured cone shifts can easily be improved by an order of magnitude with additional extinction of the background signal (at longer wavelengths with respect to resonance) and a larger field of view for precise density diagnosis. Time resolving the long wavelength Cerenkov radiation cutoff, which is a function of $N_e/2N_{cr}$, can give plasma blowout information. Since the Stark shift is quadratic with field strength, the short wavelength cutoff offers intriguing possibilities to measure large field gradients and, in general, permits studies of atoms in extremely high fields.

ACKNOWLEDGMENTS

We thank M. S. Zolotorev, B. Shadwick, L. Archambault, M. Dickinson, and S. DiMaggio for their contributions. This research was funded by the DOE, Grant Nos. DE-AC-03-76SF0098, DE-AC03-76SF00515, DE-AC-03-76SF0098, and DE-FG03-98-DP-00211, and NSF Contract No. ECS9617089.

[1] For a review, see E. Esarey *et al.*, IEEE Trans. Plasma Sci. **24**, 252 (1996).
[2] J. B. Rosenzweig, Phys. Rev. A **44**, 6854 (1991); N. Barov *et al.*, Phys. Rev. Lett. **80**, 81 (1998).
[3] M. J. Hogan *et al.*, Phys. Plasmas **7**, 2241 (2000).
[4] G. Hairapetian *et al.*, Phys. Rev. Lett. **72**, 2403 (1995); R. Govil *et al.*, *ibid.* **83**, 3202 (1999).
[5] D. H. Whittum, A. M. Sessler, and J. M. Dawson, Phys. Rev. Lett. **64**, 2511 (1990).
[6] J. Yoshii *et al.*, Phys. Rev. Lett. **79**, 4194 (1997).
[7] W. K. H. Panofsky and M. Phillips, *Classical Electricity and Magnetism* (Addison-Wesley, Reading, MA, 1962).
[8] M. A. Piestrup *et al.*, Appl. Phys. Lett. **28**, 92 (1976).
[9] V. V. Goloviznin, D. Oepts, and M. J. van der Wiel, Nucl. Instrum. Methods Phys. Res. A **393**, 510 (1997).
[10] J.-H. You *et al.*, Astron. Astrophys. **362**, 762 (2000).
[11] C. R. Vidal *et al.*, J. Appl. Phys. **40**, 3370 (1969).
[12] P. Muggli *et al.*, IEEE Trans. Plasma Sci. **27**, 791 (1999).
[13] S. DiMaggio *et al.*, in *Proceedings of 1999 Particle Accelerator Conference*, New York, edited by A. Luccio and W. MacKay (IEEE, New York, 1999), Vol. 5, p. 3705.
[14] P. Catravas *et al.*, in *Proceedings of 1999 Particle Accelerator Conference* (Ref. [13]), Vol. 3, p. 2111.
[15] *AIP Handbook*, edited by D. E. Gray (McGraw-Hill, New York, 1972).
[16] The best fit required a 20 °C offset between the measured external and actual internal oven temperature. However, this offset had little effect on the slope.
[17] R. Siemann, SLAC Tech Report No. ARDB-221 (2000).
[18] C. Clayton *et al.* (unpublished).
[19] M. S. Zolotorev (private communication).
[20] K. J. Kim, in *Physics of Particle Accelerators*, edited by Melvin Monan and Margaret Dienes, AIP Conf. Proc. No. 184 (AIP, New York, 1989), pp. 565–632.
[21] Simulations for optimized parameters of the beam-plasma interaction predict electric fields of 100 MeV/m over the bulk of the *e* beam and magnetic fields ranging from 2 T to >15 T at pinches. Self-fields from the *e* beam are below 400 MeV/m. The Stark shift for the $2S^{1/2}$ to $2P^{1/2}$ transition of Li is reported in the literature [L. R. Hunter *et al.*, Phys. Rev. A **44**, 6140 (1991)] to be 4.062 kHz/(kV/cm)^2; Zeeman shifts are 28 GHz/T.